Arab J Sci Eng (2017) 42:201–208
DOI 10.1007/s13369-016-2254-8

RESEARCH ARTICLE - CHEMISTRY

Comparison of the Physical Characteristics of Green-Synthesized and Commercial Silver Nanoparticles: Evaluation of Antimicrobial and Cytotoxic Effects

Palanivel Velmurugan[1] · Sung-Chul Hong[2] · Adithan Aravinthan[3] · Seong-Ho Jang[2] · Pyong-In Yi[2] · Young-Chae Song[4] · Eun-Sang Jung[2] · Je-Sung Park[2] · Subpiramaniyam Sivakumar[2]

Received: 29 December 2015 / Accepted: 19 June 2016 / Published online: 4 July 2016

Abstract We investigated a novel green route synthesis of silver nanoparticles (AgNPs) using watermelon rind powder extract (WR-AgNPs) as a reducing and capping agent. The efficiency of nanoparticle synthesis was evaluated by comparing the structure, functional groups, antibacterial activity, and cytotoxic effects with commercial AgNPs (C-AgNPs). The AgNP production was initially confirmed based on color changes and wavelength scanning by ultraviolet–visible spectra, which exhibited a surface plasmon resonance peak at 450 nm. We used energy-dispersive spectroscopy to confirm silver and sample purity of both experimental and commercial AgNPs from 2 to 4 keV. Fourier transform infrared spectroscopy analysis showed that the AgNPs were reduced and capped with biomolecules from functional groups in the watermelon powder extract. Further, the analysis showed that the synthesized AgNPs were similar to C-AgNPs. The morphology and crystalline nature of both AgNPs were determined using high-resolution transmission electron microscopy and X-ray powder diffraction. In addition, the synthesized and commercial AgNPs were subjected to antibacterial and cytotoxicity assays. Three-way ANOVA indicated that treatments for WR-AgNPs or C-AgNPs as well as concentration and time had significant effects on *Brevibacterium linens* and *Staphylococcus epidermidis*—an odor-causing bacteria. With respect to cytotoxic effects, 67 % cell death was observed with high concentrations (10 mg/L) of both AgNPs.

Keywords Watermelon rind · Silver nanoparticles · Characterization · Antimicrobial · Cytotoxic assay

1 Introduction

Recent research concerning the phyto-mediated synthesis of metal nanoparticles has received increased attention because this technique is low cost, eco-friendly, rapid, and has high substrate availability. This approach is an alternative that avoids environmental pollution caused by various solvents and reagents used in the physical and chemical methods of nanoparticle synthesis. Although there are several metal nanoparticles, silver nanoparticles (AgNPs) have a prominent place in biological tagging as well as the pharmaceutical and optoelectronics fields due to their unique properties. Many conventional methods such as chemical, electrochemical, and sonochemical have been used to synthesize AgNPs. Recently, green and eco-friendly methods using microbes, plant extracts, and agriculture waste have been used to synthesize AgNPs [1–3]. Enhanced antimicrobial activity of AgNPs was achieved when they were synthesized by physical, chemical, phytochemical, biological, and agro-industrial waste modes [4–6]. In particular, the agro-industrial waste method of AgNP synthesis has special applications in vari-

Palanivel Velmurugan and Sung-Chul Hong have contributed equally to this work.

✉ Subpiramaniyam Sivakumar
ssivaphd@yahoo.com

1 Division of Biotechnology, Advanced Institute of Environmental and Bioscience, College of Environmental and Bioresource Sciences, Chonbuk National University, Iksan, Jeonbuk, 570-752, Republic of Korea

2 Department of Bioenvironmental Energy, College of Natural Resource and Life Science, Pusan National University, Miryang-si, Gyeongsangnam-do, 627-706, Republic of Korea

3 College of Veterinary Medicine, Biosafety Research Institute, Chonbuk National University, Iksan 570-752, Republic of Korea

4 Department of Environmental Engineering, Korea Maritime and Ocean University, Busan, Republic of Korea

ous fields because they are low toxicity and environmentally friendly. They are also less expensive than other synthesis methods [7,8].

In general, agricultural waste is rich in polyphenols, lignins, and pectin. Therefore, previous studies have evaluated banana peels [9], custard apple peels [10], *Annona squamosa* peel extract [11], *Punicagranatum peels* [12], *Citrus sinensis peel* extract [13], and orange peel extract [14] for use in the synthesis of AgNPs. Lakshmipathy et al. [15] previously reported the synthesis of palladium nanoparticles using watermelon rind (*Citrullus lanatus*) powder extract. However, there is no report available for the synthesis of AgNPs. Watermelon, *Citrullus lanatus* (Thunb.), is a member of the cucumber family (*Cucurbitacea*). It is a large, oval, round, or oblong tropical fruit. Hydroxyl (cellulose) and carboxylic (pectin) functional groups in watermelon rind (WR) powder extract are rich in carotenoids, pectin, proteins, citrulline, and cellulose [15] content. Therefore, this study aimed to synthesize silver nanoparticles using WR powder extract. The resulting nanoparticles were then characterized by antibacterial and cytotoxicity evaluation. Further, the activity of the synthesized AgNPs was evaluated in comparison with C-AgNPs.

Antibacterial evaluation was done utilizing the known ability of some bacteria to break down specific amino acids. Bacteria such as *Brevibacterium linens* and *Staphylococcus epidermidis*, for example, are present in sweat and are known to degrade amino acids resulting in body odor. *B. linens* breaks down the amino acid methionine, present in sweat, into the gas methanethiol. Similarly, *S. epidermidis* creates body odor by converting the leucine present in sweat into isovaleric acid (3-methyl butanoic acid) [16,17]. Therefore, these bacteria could be used to compare the microbial control capacity of the AgNPs to that of commercial AgNPs (C-AgNPs). Cytotoxicity studies, on the other hand, can assess the toxicity of the nanoparticles because it damages the cell mitochondria and DNA. This is followed by oxidative stress and the induction of apoptosis [18]. Previous work has used various cell lines to analyze the cytotoxicity of AgNPs including NIH 3T3 fibroblasts, HeLa cells, human breast cancer MCF-7 cells, and glioblastoma cells as well as rat splenocytes [18]. In this study, AgNPs synthesized via a watermelon rind-mediated process (WR-AgNPs) and commercial silver nanoparticles (C-AgNPs) were subjected to a cytotoxicity evaluation using rat splenocytes.

2 Experimental Methods

2.1 Extract Preparation and AgNP Synthesis

Commercial silver nanopowder was purchased from Sigma-Aldrich, USA. The powder had a size of <100 nm and was composed of 99.5 % metals; details are given on the Sigma-Aldrich Web site. The synthesis of nanoparticles separated the rind of a single watermelon and washed it with sterile nanopure water (18 $\mu\Omega$/m conductivity, less than 3 ppb TOC) (Barnstead, USA) and oven-dried at 60 °C. The sample was then powdered using a mechanical blender.

An extract was prepared by boiling 10 g of resulting WR powder in 100 mL of nanopure water for 30 min in a heating mantle followed by filtration. Then, 1 mM silver nitrate (45 mL) ($AgNO_3-$) (Sigma-Aldrich, St. Louis, MO, USA) was added to the extract (5 mL). The silver nitrate reduction was monitored colorimetrically from light yellow to yellowish dark brown. The product was then separated from the sample by 15 min centrifugation (15,000 rpm) followed by freeze-drying.

2.2 Characterization of Synthesized and C-AgNPs

The samples that successfully changed color were scanned with UV–Vis spectrophotometer between 300 and 700 nm wavelength range (Shimadzu, UV-1800, Japan) using a dual beam operated at a 1 nm resolution. Scanning electron microscopy and energy-dispersive spectra (SEM–EDS) (JEOL-64000, Japan) confirmed the elemental composition of the nanoparticles. The acceleration voltage and emission current were 15 kV and 12 μA, respectively, from a cold field emission gun. Small amounts of sample were dropped on a carbon-coated copper grid followed by gold coating to prepare thin films. The films were dried with a mercury lamp for 5 min. Small amount of water-dispersed nanoparticles were dropped onto a copper disk and evaporated at room temperature. The copper disk was subsequently attached to a brass sample holder using carbon tape. Fourier transform infrared (FTIR) spectra of both types of AgNPs were acquired from PerkinElmer instrument (Norwalk, CT, USA) in the diffuse reflectance mode operating at 4 cm^{-1} via KBr pellets. The surface morphology and size distribution of nanoparticles were observed with high-resolution transmission electron microscopy (HR-TEM) (JEOL, JEM-2010HR, West Chester, PA, USA). An X-ray diffractometer (XRD) (Rigaku, Japan) was used for X-ray powder diffraction of AgNPs with 2θ scans from 30° to 80° at 0.04° per min with a time constant of 2 s.

2.3 Antibacterial Activity of WR- and C-AgNPs

The odor-causing bacterial strains (*B. linens*-KACC-14346 and *S. epidermidis*-KACC-13234) were purchased (Korean agriculture culture collection, South Korea) and inoculated into nutrient broth medium. A shaking incubator was used for incubation (37 °C for 48 h). After incubation, cultures were grown in 50 mL of nutrient broth containing the WR-AgNPs or C-AgNPs at concentrations ranging from 20 to 160 μg. An

appropriate control without AgNPs was also included. The bacterial growth was determined with a spectrophotometer with an optical density measurements every 4 h. Three replicates were used for each concentration. Three-way ANOVA was employed to test the effects of three variables: treatments (treatment with WR-AgNPs or treatment with C-AgNPs), AgNP concentration, and time.

2.4 Sample Preparation for Cytotoxicity Assay

The animal experiments were carried out in rats after approval of the institutional animal care and Chonbuk National University committee ethics. Preparation of the rat splenocytes and the 3-(4,5-dimethylthiazol-2-yl)-2,5-diphenyltetrazolium bromide assay has been previously described by Arvinthan et al. [18]. Briefly, adult rats (2–3 months old; Sprague–Dawley) were purchased from Koatech, South Korea, and kept in a pathogen-free environment. The utmost care was taken to collect fresh splenocytes from the rat spleen as described by Lu et al. [19]. Rat spleens were then used to prepare single-cell suspensions. The rat spleen tissue was pressed with a sterile wire mesh, and the cells were then washed with 1 % antibiotic solution (RPMI, Gibco, Anti–Anti, South Korea). Further, the isolated splenocytes were treated with 0 to 10 mg/L of both AgNPs in 96-well tissue culture plates. Finally, the plates were incubated at 37 °C for 1 day with 5 % CO_2. The incubated cells were then used for the 3-(4,5-dimethylthiazol-2-yl)-2,5-diphenyltetrazolium bromide (MTT) assay. The 20 μL of MTT was prepared from stock (5 mg/mL, yellow tetrazole) and were added to each AgNP-treated well and then incubated for 4 h. After incubation, purple-colored formazan crystals were observed in the bottom of the well. These crystals were mixed with dimethyl sulfoxide (200 μL, DMSO) and read by multi-well plate reader at 595 nm (Biotek, Epoch microplate spectrophotometer, Winooski, USA). Three replicates were used for each concentration. Analysis of variance (one-way ANOVA) evaluated the significance of the observed differences in the growth of rat splenocytes between the control, C-AgNP, and the treatment, WR-AgNP, groups. The degree of significance ($*p < 0.05$; $**p < 0.01$; $***p < 0.001$) is indicated when appropriate.

3 Results and Discussion

3.1 Characterization Studies

The reduction of pure Ag^+ ions to Ag^0 was indicated by a visual color change (light yellow to brown). Then, the UV–visible absorbance of the reaction mixture was scanned between 300 and 700 nm. The color change and size differences were based on the concentration and ratio of the

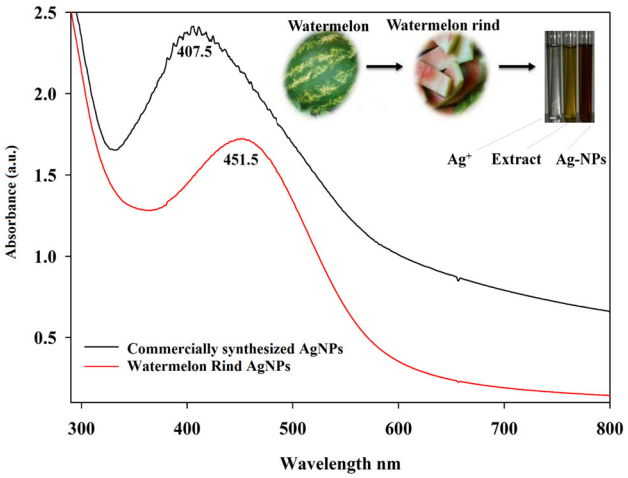

Fig. 1 UV–Vis absorption spectrum of watermelon AgNPs. The insert shows the protocol

reducing material [20]. This color change is due to the excitation of surface plasmon resonance (SPR). Figure 1 shows the surface plasmon vibrations of AgNPs (450 nm), and the inset shows a watermelon fruit, WR, a silver solution, the rind extract, and colloidal silver. The SEM-EDS spectra revealed the elemental nature of the synthesized C-AgNPs, and the results are shown in Fig. 2a, b. EDS data in Fig. 2a, b show a nanoparticle secondary electron image and the corresponding X-ray spectrum that was generated from the selected SEM scanning area. The number of X-ray events (counts) is plotted on the *Y*-axis, and energy is plotted on the *X*-axis.

The elemental silver phases have a signature peak at 3 keV for both nanoparticles. Some weaker peaks were also found for the synthesized AgNPs that correspond to carbon and oxygen. This might have originated from the WR extract. There was also a strong signal for the coating agent (gold, Au) in the EDS data. This results from the copper substrate. The major peaks in FTIR spectra of both AgNPs (shown in Fig. 3a, b) exhibit various wave numbers that correspond to different functional groups. The strong peak at 3, 385 cm^{-1} and peaks at 2927 and 2852 cm^{-1} correspond to the symmetrical stretching vibrations of the –OH groups of hydroxyl molecules and vibrations of methyl and methoxy groups, respectively. The peaks at 1652 and 1390 cm^{-1} correspond to bending vibrations of –OH groups and carboxylate groups. A strong peak at 1, 052 cm^{-1} corresponds to the C–O–C vibration band. These results were consistent with a previous study of the synthesis of palladium nanoparticles using WR powder extract [15]. Based on the observed functional groups, the results confirm the presence of polyhydroxyl groups from the WR powder extract bound to the AgNPs. The synthesized and commercial nanoparticle peaks are similar.

TEM images of AgNPs are shown in Fig. 4a–h. Both nanoparticles under TEM showed a circular and oval shape

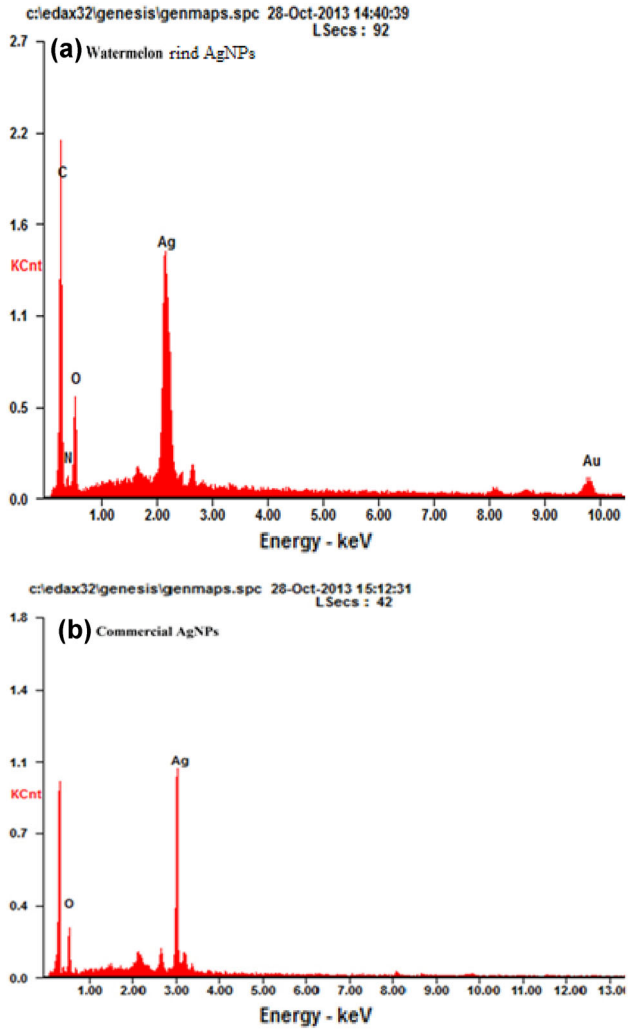

Fig. 2 SEM–EDS spectra of **a** watermelon AgNPs and **b** commercial AgNPs

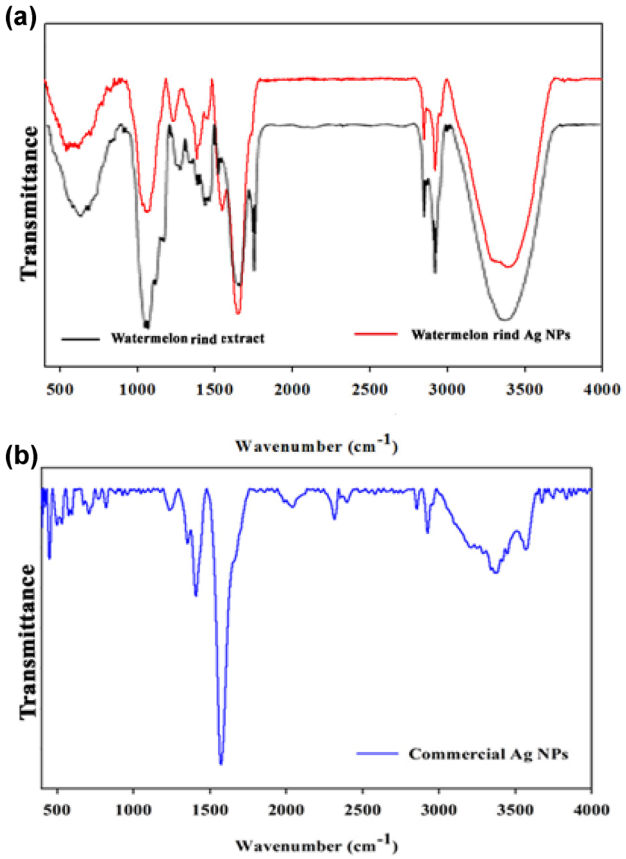

Fig. 3 FTIR spectra of **a** watermelon AgNPs and **b** commercial AgNPs

with smooth edges (Fig. 4a, e) in the nanoparticles ranges between 10 and 50 nm (Fig. 4b, f). The fringe spacing was also comparable for both nanoparticles, and measured 0.22 nm between lattice planes to the (1 1 1) lattice spacing of face-centered cubic (fcc) silver ($d_{1\,1\,1} = 0.2359$ nm) (Fig. 4c, g). The SAED pattern exhibited bright circular spots that corresponded to (1 1 1), (2 0 0), (2 2 0), and (3 1 1) (Fig. 4d, h). The crystalline nature of both AgNPs was further confirmed via the Bragg reflection planes. These results are consistent with those previously reported [21].

The XRD pattern of the nanoparticles is shown in Fig. 5a, b. The prominent diffraction peaks at $2\theta = 37.8$, 46.3, 66.2 and 77.92 were attributed to the diffraction of (111), (200), (220), and (311) planes for C-AgNPs. For WR-AgNPs, the peaks at $2\theta = 32.8$, 46.3, 66.2, and 77.92 were attributed to the diffraction of (111), (200), (220), and (311) planes. All of the above peaks were compared to the standard powder diffraction card (Joint Committee on Powder Diffraction Standards—JCPDS, No. 04-0783). All diffraction peaks clearly indexed the cubic crystal structure of both AgNPs. The minor diffraction peaks at $2\theta = 28.4$, 55.6, 48.4 may originate from the binding of WR powder extract precursors to the AgNPs (Fig. 5a). Similar diffraction peaks were also observed in previous studies that used green [3,22–24] and chemically synthesized [25,26] AgNPs.

3.2 Antibacterial and Cytotoxicity Assays

Previous reports highlighted the potential of green-synthesized AgNPs to inhibit bacteria and fungi [2,7]. However, the inhibitory effect of AgNPs should be evaluated carefully prior to its use as an antimicrobial. In our study, the antibacterial activity of synthesized and C-AgNPs was studied by determining their activity against two odor-causing pathogens, *B. linens* and *S. epidermidis*. The bacteria were inoculated into nutrient broth containing different concentrations of both nanoparticles. The cultures were monitored for growth at regular time intervals for 0–24 h, and the OD values are shown in Fig. 6a, b for WR-AgNPs and Fig. 6c, d for C-AgNPs. The growth of both bacteria increased with increasing incubation times in the control medium as well as

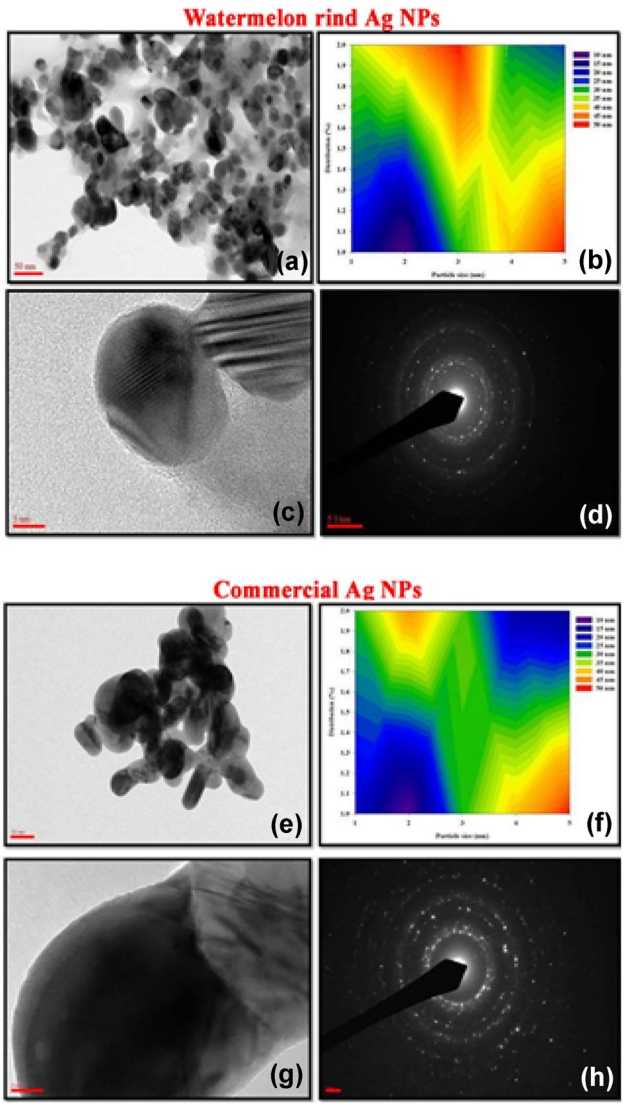

Fig. 4 HR-TEM images of watermelon AgNPs (**a**–**d**) and commercial AgNPs (**e**–**h**)

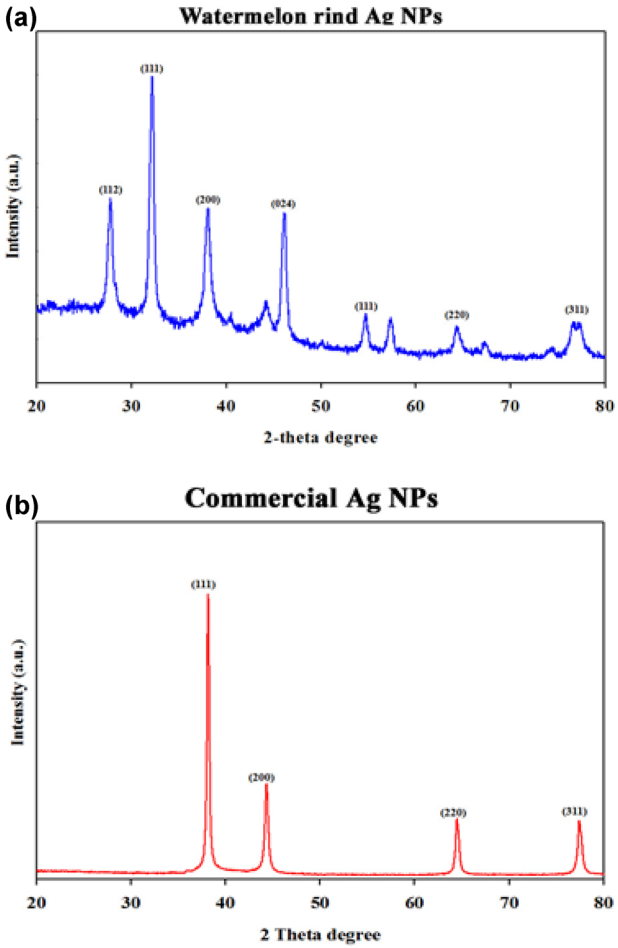

Fig. 5 XRD patterns of **a** watermelon AgNPs and **b** commercial AgNPs

in the WR-AgNP- and C-AgNP-containing medium. However, the increase in growth that was observed for either AgNP treatments was smaller than that observed for the control. The growth of both bacteria decreased with increasing concentrations of both AgNPs. The results of three-way ANOVA analysis for both the *B. linens* and *S. epidermidis* experiments and both AgNPs showed significant differences within treatments and between treatments (Table 1). These results are consistent with previous studies on the inhibitory effect of AgNPs antibacterial activity against human skin pathogens obtained from *Pinus densiflora* extracts [27].

The cytotoxic potential of nanoparticles was assessed by MTT assay. Figure 7a, b (and inserts) shows that increasing concentrations (2–10 mg/L) of both AgNPs reduced splenocyte viability. The reduction in color at 595 nm versus untreated cells highlights the cytotoxicity of the nanoparticles. The *in vitro* cytotoxicity of different concentrations (2–10 mg/L) of WR-AgNPs is shown in Fig. 7a, and the insert image shows the observed cell death. Figure 7b and the insert show the cell viability and observed cell death after treatment with C-AgNPs. Ten percent of cell death was observed at 2 mg/L. The viability decreased increasing concentrations of AgNPs. It reached 67 % at 10 mg/L. Several previous reports have demonstrated that the cytotoxicity of AgNPs was determined by the concentration of the nanoparticles [18,28].

3.3 Probable Reduction and Capping Mechanism

Watermelon rind contains high concentrations of most nutrients including total phenol, antioxidants, flavonoids, citrulline, and lycopene. These were identified as the major components in watermelon rind [29]. The reduction reaction is due to the presence of two hydroxyl groups in the benzene ring. In the proposed reaction mechanism, Ag^{+} first forms an intermediate silver complex and then forms silver ions and

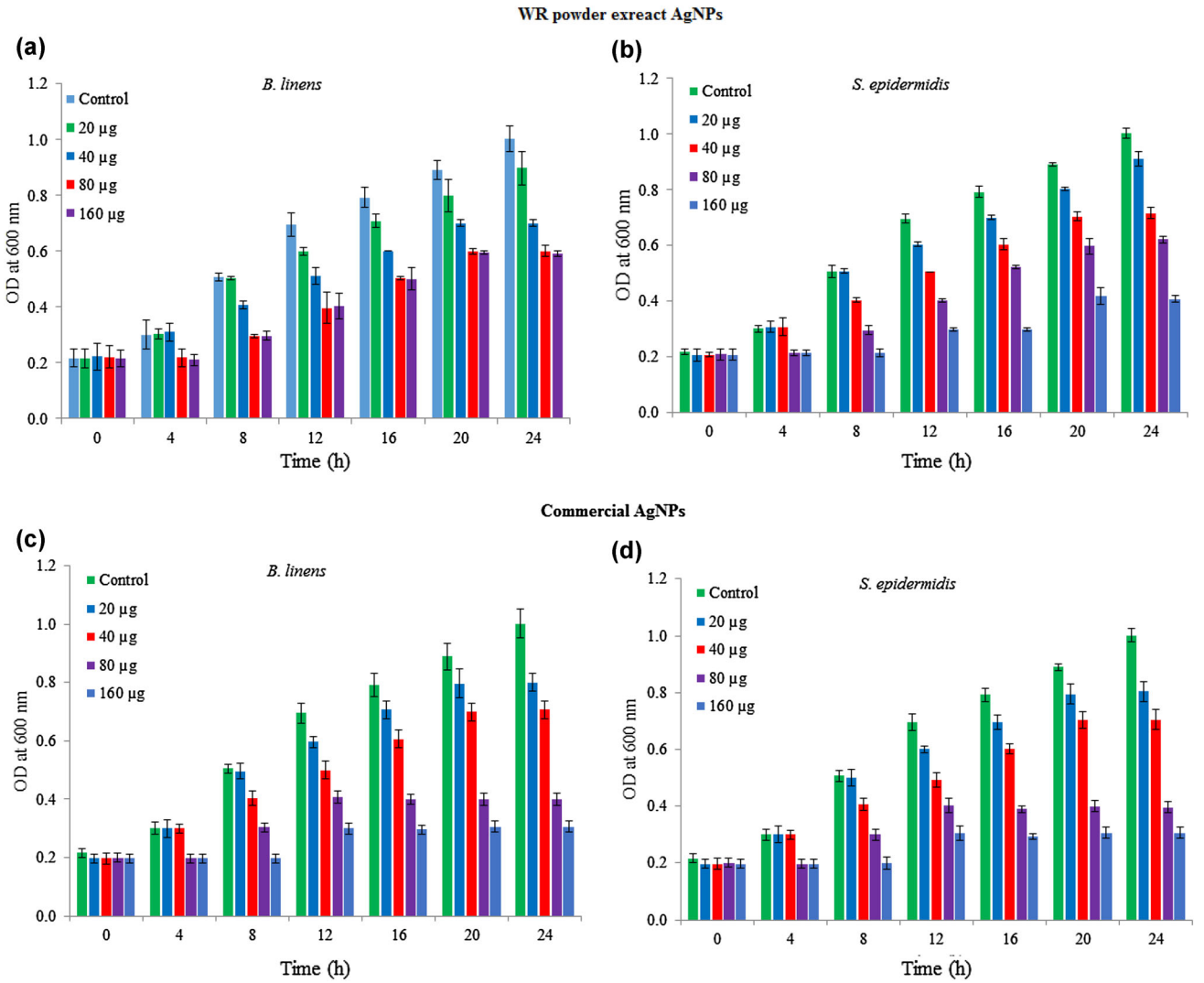

Fig. 6 Effect of watermelon AgNPs on the growth of **a** *B. linens* and **b** *S. epidermidis*, and the effect of commercial AgNPs on **c** *B. linens* and **d** *S. epidermidis*. The results are presented as the mean values of three replicate samples for each treatment. The *error bars* indicate the standard deviation ($n = 3$)

Table 1 Statistical analysis of the growth of *B. linens* and *S. epidermidis* via three-way ANOVA (*F* values) with three variables (treatment, concentration, and time)

Source	*df*	Growth	
		B. linens	*S. epidermidis*
Treatment (WR-AgNPs and C-AgNPs)	1	128*	67*
Time	6	1155*	1688*
Concentration	4	701*	1402*
Treatment × time	6	14*	14*
Treatment × concentration	4	40*	17*
Time × concentration	24	41*	83*
Treatment × time × concentration	24	5*	4*

* $P < 0.05$

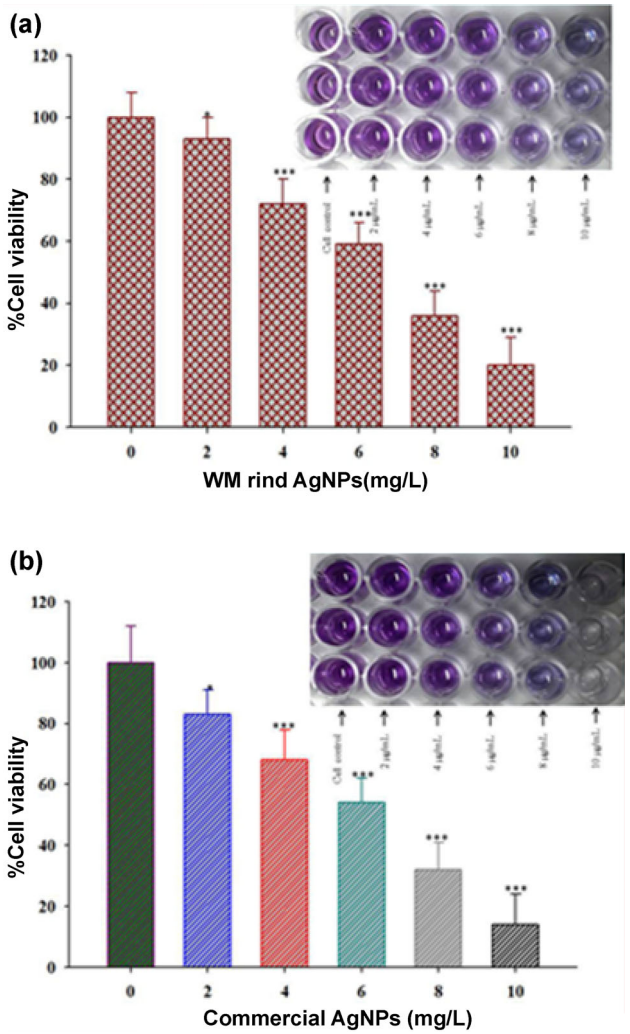

Fig. 7 Cytotoxic effect of **a** synthesized and **b** commercial AgNPs on the growth of rat splenocytes. The *inserts* show images of control and dead cells. A dose-dependent reduction in cell viability was observed at 595 nm. The *error bars* indicate the standard deviation ($n = 3$). The *stars* above the *error bar* indicate significant differences versus the control ($*p < 0.05$; $***p < 0.001$)

quinone [30]. These free Ag^+ ions are reduced to AgNPs using free electrons or nascent hydrogen that is produced in the process. The AgNPs have a negative zeta potential value in their pure form [31]. The possible capping mechanism of polyphenolic compounds is the interaction of hydrogen atoms in polyphenolic compounds from the watermelon rind extract with Ag nanoparticles.

4 Conclusion

In this manuscript, we describe a green synthetic approach for the synthesis of AgNPs that employs an easy and low-cost method that does not use any toxic chemicals and is rich in the availability of eco-friendly material (WR powder). The HR-TEM and XRD data indicate that both commercial and synthesized AgNP particles were similar in shape and size. The antimicrobial activity and cytotoxicity assays, however, showed that the C-AgNPs exhibited stronger activity than the green-synthesized AgNPs. The microbial growth inhibition of biologically synthesized AgNPs and C-AgNPs was comparable. These results indicate that the AgNPs obtained through WR powder extract-mediated synthesis have immense potential and might have a notable impact on the pharmaceutical, textile, biomedical, and cosmetic industries. In addition, these AgNPs could become an alternative to chemically synthesized AgNPs.

Acknowledgments This work was supported by a two-year research grant of Pusan National University.

References

1. Velmurugan, P.; Shim, J.; Balachander, V.; Kamala-Kannan, S.; Lee, K.J.; Oh, B.T.: Crystallization of silver through reduction process using *Elaeis guineensis* biosolid extract. Biotechnol. Prog. **27**, 273–279 (2011)
2. Velmurugan, P.; Iydroose, M.; AbdulKader Mohideen, M.H.; Mohan, T.S.; Cho, M.; Oh, B.T.: Biosynthesis of silver nanoparticles using *Bacillus subtilis* EWP-46 cell-free extract and evaluation of its antibacterial activity. Bioprocess Biosyst. Eng. **37**, 1527–1534 (2014)
3. Velmurugan, P.; Cho, M.; Lim, S.S.; Seo, S.K.; Myung, H.; Bang, K.S.; Sivakumar, S.; Cho, K.M.; Oh, B.T.: Phytosynthesis of silver nanoparticles by *Prunus yedoensis* leaf extract and their antimicrobial activity. Mater. Lett. **138**, 272–275 (2015)
4. Reddy, V.; Torati, R.S.; Oh, S.; Kim, C.G.: Biosynthesis of gold nanoparticles assisted by *Sapindus mukorossi* Gaertn. Fruit pericarp and their catalytic application for the reduction of *p*-nitroaniline. Ind. Eng. Chem. Res. **52**, 556–564 (2013)
5. Velmurugan, P.; Cho, M.; Lee, S.M.; Park, J.H.; Bae, S.; Oh, B.T.: Antimicrobial fabrication of cotton fabric and leather using green-synthesized nanosilver. Carbohyd. Polym. **106**, 319–325 (2014)
6. Dauthal, P.; Mukhopadhyay, M.: Agro-industrial waste-mediated synthesis and characterization of gold and silver nanoparticles and their catalytic activity for 4-nitroaniline hydrogenation. Korean J. Chem. Eng. **32**, 837–844 (2015)
7. Lee, K.J.; Park, S.H.; Govarthanan, M.; Hwang, P.H.; Seo, Y.S.; Cho, S.; Lee, W.H.; Lee, J.Y.; Kamala-Kannan, S.; Oh, B.T.: Synthesis of silver nanoparticles using cow milk and their antifungal activity against phytopathogens. Mater. Lett. **105**, 128–131 (2013)
8. Ahmad, A.; Mukherjee, P.; Senapati, S.; Mandal, D.; Khan, M.I.; Kumar, R.; Sastry, M.: Extracellular biosynthesis of silver nanoparticles using the fungus *Fusarium oxysporum*. Colloids Surf. B Biointerfaces **28**, 313–318 (2003)
9. Bankar, A.; Joshi, B.; Kumar, A.R.; Zinjarde, S.: Banana peel extract mediated novel route for the synthesis of silver nanoparticles. Colloids Surf. A. Physicochem. Eng. Asp. **368**, 58–63 (2010)
10. Roopan, S.M.; Bharathi, A.; Kumar, R.; Khanna, V.G.; Prabhakarn, A.: Acaricidal, insecticidal, and larvicidal efficacy of aqueous extract of *Annona squamosa* L peel as biomaterial for the reduction of palladium salts into nanoparticles. Colloids Surf. B. Biointerfaces **92**, 209–212 (2012)

11. Kumar, R.; Roopan, S.M.; Prabhakarn, A.; Khanna, V.G.; Chakroborty, S.: Agricultural waste *Annona squamosa* peel extract: biosynthesis of silver nanoparticles. Spectrochim. Acta A. Mol. Biomol. Spectrosc. **90**, 173–176 (2012)
12. Edison, T.J.; Sethuraman, M.G.: Biogenic robust synthesis of silver nanoparticles using *Punica granatum* peel and its application as a green catalyst for the reduction of an anthropogenic pollutant 4-nitrophenol. Spectrochim. Acta A. Mol. Biomol. Spectrosc. **4**, 262–264 (2013)
13. Kaviya, S.; Santhanalakshmi, J.; Viswanathan, B.; Muthumary, J.; Srinivasan, K.: Biosynthesis of silver nanoparticles using citrus sinensis peel extract and its antibacterial activity. Spectrochim. Acta A. Mol. Biomol. Spectrosc. **79**, 594–598 (2011)
14. Manal, A.A.; Awatif, A.H.; Khalid, M.O.O.; Elradi, F.A.E.; Nada, E.E.; Lamina, A.A.; Shorog, M.A.; Nada, M.M.; Abdelelah, A.G.A.: Silver nanoparticles biogenic synthesized using an orange peel extract and their use as an anti-bacterial agent. J. Nanopart. Res. **9**, 34–40 (2014)
15. Lakshmipathy, R.; Palakshi Reddy, B.; Sarada, N.C.; Chidambaram, K.; Khadeer Pasha, S.K.: Watermelon rind-mediated green synthesis of noble palladium nanoparticles: catalytic application. Appl. Nanosci. **5**, 223–228 (2015)
16. Ara, K.; Hama, M.; Akiba, S.; Koike, K.; Okisaka, K.; Hagura, T.; Kamiya, T.; Tomita, F.: Foot odor due to microbial metabolism and its control. Can. J. Microbiol. **52**, 357–364 (2006)
17. Kanlayavattanakul, M.; Lourith, N.: Body malodours and their topical treatment agents. Int. J. Cosmet. Sci. **33**, 298–311 (2011)
18. Aravinthan, A.; Govarthanan, M.; Selvam, K.; Praburaman, L.; Selvankumar, T.; Balamurugan, R.; Kamala-Kannan, S.; Kim, J.H.: Sunroot mediated synthesis and characterization of silver nanoparticles and evaluation of its antibacterial and rat splenocyte cytotoxic effects. Int. J. Nanomedicine **10**, 1977–1983 (2015)
19. Lu, L.; Hsieh, M.; Oriss, T.B.; Morel, P.A.; Starzl, T.E.; Rao, A.S.; Thomson, A.W.: Generation of dendritic cells from mouse spleen cell cultures in response to GM-CSF: immunophenotypic and functional analyses. Immunology **84**, 127–134 (1995)
20. Abdel-Halim, E.S.; El-Rafie, M.H.; Al-Deyab, S.S.: Polyacrylamide/guar gum graft copolymer for preparation of silver nanoparticles. Carbohydr. Polym. **85**, 692–697 (2011)
21. Vigneshwaran, N.; Nachane, R.P.; Balasubramanya, R.H.; Varadarajan, P.V.: A novel one-pot 'green' synthesis of stable silver nanoparticles using soluble starch. Carbohydr. Res. **341**, 2012–2018 (2006)
22. Bar, H.; Bhui, D.K.; Sahoo, G.P.; Sarkar, P.; De, S.P.; Misra, A.: Green synthesis of silver nanoparticles using latex of *Jatropha curcas*. Colloids Surf. A. Physicochem. Eng. Asp. **339**, 134–139 (2009)
23. Raveendran, P.; Fu, J.; Wallen, S.L.: Completely "green" synthesis and stabilization of metal nanoparticles. J. Am. Chem. Soc. **125**, 13940–13941 (2003)
24. Velmurugan, P.; Iydroose, M.; Lee, S.M.; Cho, M.; Park, J.H.; Balachandar, V.; Oh, B.T.: Synthesis of silver and gold nanoparticles using cashew nut shell liquid and its antibacterial activity against fish pathogens. Indian J. Microbiol. **54**, 196–202 (2014)
25. Stevenson, A.P.; Bea, D.B.; Civit, S.; Contera, S.A.; Cerveto, A.I.; Trigueros, S.: Three strategies to stabilise nearly monodispersed silver nanoparticles in aqueous solution. Nanoscale Res. Lett. **7**, 151–158 (2012)
26. Valencia, G.A.; Vercik, L.C.D.O.; Ferrari, R.; Vercik, A.: Synthesis and characterization of silver nanoparticles using water-soluble starch and its antibacterial activity on *Staphylococcus aureus*. Starch/Starke **65**, 931–937 (2013)
27. Velmurugan, P.; Park, J.H.; Lee, S.M.; Jang, J.S.; Lee, K.J.; Han, S.S.; Lee, S.H.; Cho, M.; Oh, B.T.: Synthesis and characterization of nanosilver with antibacterial properties using *Pinus densiflora* young cone extract. J. Photochem. Photobiol. B. Biol. **147**, 63–68 (2015)
28. Vivek, R.; Thangam, R.; Muthuchelian, K.; Gunasekaran, P.; Kaveri, K.; Kannan, S.: Green biosynthesis of silver nanoparticles from *Annona squamosa* leaf extract and its in vitro cytotoxic effect on MCF-7 cells. Process Biochem. **47**, 2405–2410 (2012)
29. Tarazona-Diaz, M.P.; Viegas, J.; Moldao-Martinsc, M.; Aguayo, E.: Bio-active compounds from flesh and by-product of fresh-cut watermelons cultivars. J. Sci. Food Agr. **91**, 805–812 (2011)
30. Seema, G.; Amrish, C.: Bio synthesis and anthelmintic activity of silver nanoparticles using aqueous extract of *Saraca indica* leaves. Int. J. Therap. Appl. **7**, 9–12 (2012)
31. Mohan, H.: Textbook of Pathology, 5th edn. Jaypee Brothers, New Delhi (2005)